Energy & Environmental Science

RSC Publishing

COMMUNICATION

View Article Online
View Journal | View Issue

Building multiple adsorption sites in porous polymer networks for carbon capture applications†

Cite this: *Energy Environ. Sci.*, 2013, **6**, 3559

Received 2nd July 2013
Accepted 6th September 2013

DOI: 10.1039/c3ee42226g

www.rsc.org/ees

Weigang Lu,‡[a] Wolfgang M. Verdegaal,‡[a] Jiamei Yu,[b] Perla B. Balbuena,[b] Hae-Kwon Jeong[b] and Hong-Cai Zhou*[a]

IAST calculations reveal that sulfonate ammonium salt grafting renders porous polymer networks (PPN-6-SO_3NH_4) with exceptionally high adsorption selectivity for CO_2 over N_2 and CO_2 over CH_4. Breakthrough experiments confirm the high CO_2 adsorption capacity (1.7 mmol g^{-1}, 75 mg g^{-1}) by feeding 15% CO_2 balanced with N_2 at 295 K and 1 bar.

For decades, aqueous amine solutions have been extensively used for the removal of CO_2 from natural gas or flue gas streams in coal-fired power plants. The strong chemical interaction between amine and CO_2 molecules is a double-edged sword, on the one hand, it endows the amine solutions with high capacity and selectivity for CO_2 over other small gas molecules, on the other hand, it necessitates high temperature to release the CO_2, the heat-up of aqueous solutions requires a significant amount of energy due to its high heat capacity, as a result, the regeneration cost adds up to *ca.* 30% of the power produced by the power plant.[1–3] Largely for this reason, intensive research activities have been dedicated to addressing this energy penalty issue.

Porous materials are deemed to be promising candidates to replace aqueous amine solutions because of their energy-conserving advantages, such as easily taking up and releasing CO_2, low heat capacity, as well as high gas flow rate.[4–13] A great deal of effort has been expended in recent years on exploring porous materials for this particular purpose. Though there is some progress, even the top performers are still more or less short of real practical applications.

Aside from regeneration cost, there are several other critical criteria to satisfy before porous materials can actually make their way to replace amine solutions: (1) *stability*: MgMOF-74 can reach an unprecedented working capacity of 17.6 wt%,[14] however, the effect of humidity on the performance of MgMOF-74 is discouraging, only 16% of the initial CO_2 capacity was recovered after exposure at 70% relative humidity,[15] which raised doubts on its long-term stability under harsh flue gas conditions and concerns about the added cost potentially associated with flue gas dehumidification; (2) *high CO_2 capacity*: porous materials, such as MOF-210,[16] NU-100,[17] PAF-1,[18] PPN-4,[19] and others,[12,20,21] have been deemed to be viable storage alternatives because of their high porosity and therefore significantly increased accessible contact area with gas molecules. Indeed, these materials showed the record high storage capacities at high pressures. Unfortunately only moderate CO_2 uptake capacities were observed under ambient conditions due to the weak interaction between the materials and the CO_2 gas molecules; (3) *high selectivity*: to design porous materials for separating CO_2 from other gases such as CH_4 and N_2, there are

Broader context

Massive generation of CO_2 from power plants using fossil fuels has an enormous impact on the global climate and environment. Of the many CO_2 capture strategies that have emerged, the only deployed technology in industry is "amine scrubbing". It involves absorption of CO_2 into an aqueous solution of amine at ambient temperature and regeneration of amine by stripping with hot water steam. While amine scrubbing can efficiently achieve CO_2 capture, it suffers from high parasitic energy consumption of over 30%. Moreover, the caustic and volatile nature of liquid amine absorbent has an adverse environmental impact. Porous materials are deemed to be promising candidates to address the above challenges because of their energy-conserving advantages, such as easily taking up and releasing CO_2, low heat capacity, as well as high gas flow rate. Sulfonate ammonium salt grafted porous polymer networks (PPN-6-SO_3NH_4) show exceptionally high adsorption selectivity for CO_2 over N_2 and CH_4. Breakthrough experiments confirm the high CO_2 adsorption capacity under simulated flue gas conditions. The resulting outcome of this technology development effort will be a significant increase in CO_2 capture capacity and reduction in gas separation costs which will provide an advanced alternative to "amine scrubbing".

[a]*Department of Chemistry, Texas A&M University, College Station, TX, 77843, USA. E-mail: zhou@mail.chem.tamu.edu; Fax: +1-979-845-1595; Tel: +1-979-422-6329*

[b]*Artie McFerrin Department of Chemical Engineering, Texas A&M University, College Station, TX 77843-3122, USA*

† Electronic supplementary information (ESI) available: Isotherm fit, IAST calculation, and breakthrough calculation. See DOI: 10.1039/c3ee42226g

‡ The first and second authors contributed equally to this research.

two important parameters we have to keep in mind; one is CO_2 gas molecules having relatively small kinetic diameter (3.3, 3.6, and 3.8 Å for CO_2, CH_4, and N_2, respectively)[22] and the other is CO_2 gas molecules having much larger quadrupole moment,[23] which causes CO_2 gas molecules to have much higher polarizability, therefore much stronger electrostatic interactions with sorbents. An obvious strategy to provide both the aforementioned properties is to incorporate functionalities, which could possibly reduce each cavity to better match the size of CO_2 gas molecules; more importantly, the added strong adsorption sites can greatly boost CO_2 adsorption capacity,[24–30] although it will also help N_2 and CH_4 adsorption capacities to some extent, it could easily be offset by the loss of surface area due to the incorporated functionalities taking up space. For example, the CO_2 adsorption capacity of PPN-6-CH_2EDTA is lower than that of MgMOF-74 at low pressures, but its N_2 adsorption capacity is much lower because of its much smaller surface area; in all, PPN-6-CH_2EDTA has much higher CO_2/N_2 adsorption selectivity.[31]

Porous polymer networks (PPNs), a class of purely organic materials with surface areas comparable to metal–organic frameworks (MOFs), exhibit much higher physicochemical stability due to covalent bonding in the network construction;[32] this, despite the fact that most of them are amorphous, is desirable in practical applications. On the other hand, PPNs are superior to other amorphous materials, such as porous carbons, in terms of interaction with gas molecules. The frequent utilization of aromatic rings lends PPNs with high adsorption enthalpy for CO_2 due to the uneven distribution of electron density in the aromatic system; moreover, the introduction of functionalities is feasible because aromatic rings are known for their susceptibility to organic reactions, such as electrophilic aromatic substitutions.

Previously we have reported the synthesis of sulfonate-grafted PPNs (PPN-6-SO_3H and PPN-6-SO_3Li);[33] their preferential CO_2 adsorption at low pressures can be attributed to the reduced pore size and added strong adsorption sites (sulfonate groups). To further increase the CO_2 adsorption capacity at low pressures, an intuitive approach is to construct multiple strong adsorption sites, as in the case of PPN-6-SO_3Li,[33] in which the lithium cation can be viewed as an added adsorption site for CO_2. Aside from metal cations, N-containing groups have been intensively studied for this particular purpose due to their basicity.

Here we report the synthesis of PPN-6-SO_3NH_4 by simply mixing PPN-6-SO_3H and ammonia hydroxide (Scheme 1). The as-synthesized sample was washed thoroughly with methanol and water, and then dried under high vacuum at 120 °C for 10 hours prior to any characterization and measurements. Elemental analysis confirmed the quantitative conversion (Table S5†). The added merits of forming sulfonate ammonium salt in PPN are two-fold: (1) the added NH_4 moiety is a strong binding site for CO_2, as evident in its much higher CO_2 adsorption capacity at lower pressures (Fig. 1b); (2) the basicity of the amine group is significantly reduced owing to electron delocalization to the p orbital of sulfur, therefore no chemical interaction (between CO_2 and ammonia) was observed, as evident in its reversible CO_2 isotherms and no obvious hysteresis loops (Fig. S11†).

As a result of the incorporation of a NH_4 moiety, the surface area of PPN-6-SO_3NH_4 continues to drop significantly to 593 m^2 g^{-1}, which indeed is only about half of that of PPN-6-SO_3H (Fig. 1a). However, at 0.15 bar and 295 K, PPN-6-SO_3NH_4 has the highest CO_2 adsorption capacity (Fig. 1b), which suggests that the CO_2 adsorption capacity is determined by the number of strong adsorption sites at low pressures; as pressure goes up, strong adsorption sites are all occupied, and surface area weighs in. The three sulfonate-functionalized PPNs end up with similar CO_2 adsorption capacity at 1.0 bar.

The strong interaction between CO_2 and sorbents can be quantified with adsorption enthalpy, as calculated from variable-temperature CO_2 isotherms. As we can see from Fig. 2a, PPN-6-SO_3NH_4 has −40 kJ mol^{-1} adsorption enthalpy at zero-loading, which is comparable to other top-performing materials in the literature, such as Mg-MOF-74 (−39 kJ mol^{-1})[34] and NaX (−43 kJ mol^{-1}).[34] These values fall well within the range of what is considered to be an ideal adsorption enthalpy for CO_2 scrubbing from flue gas.[35] Under ambient conditions, low CO_2 adsorption enthalpy leads to low CO_2 adsorption capacity at low pressure and low CO_2 over N_2 selectivity, while higher enthalpies will raise regeneration costs because of the energy input required for the reverse process; extra energy is needed to break up the strong binding between the adsorbent and CO_2, as in the case of 30% MEA solution, which has −84 kJ mol^{-1} adsorption enthalpy,[34] and is very efficient in terms of CO_2 capture due to the chemisorption nature, however, it is also very difficult to be fully regenerated. Thus, a balance has to be struck

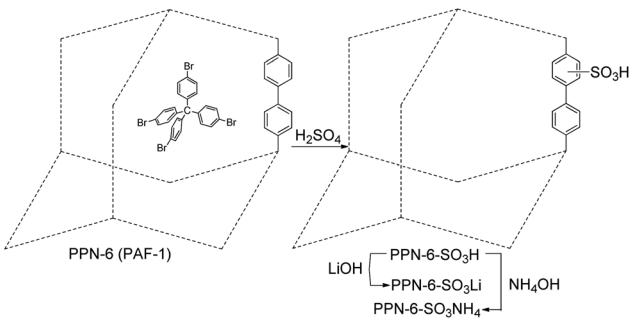

Scheme 1 Synthetic route for sulfonate functionalized PPNs.

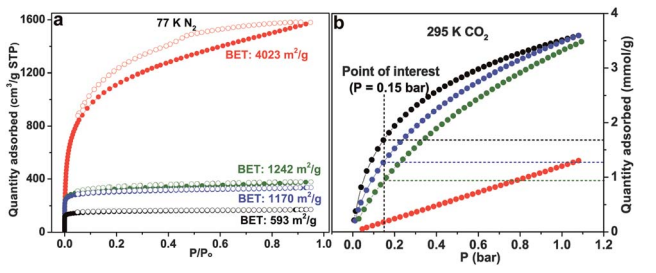

Fig. 1 (a) 77 K N_2 sorption isotherms, adsorption (●)/desorption (○); (b) 295 K CO_2 adsorption isotherms. PPN-6 (red), PPN-6-SO_3H (green), PPN-6-SO_3Li (blue), and PPN-6-SO_3NH_4 (black).

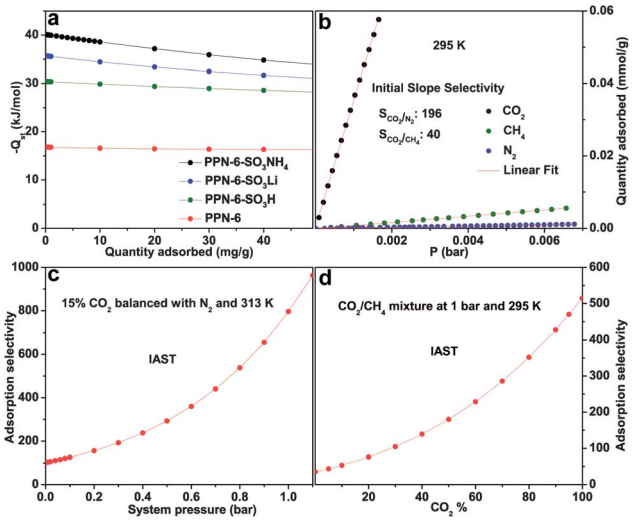

Fig. 2 (a) Adsorption enthalpy Q_{st}, as calculated with adsorption curves at three different temperatures; (b) adsorption selectivity of CO_2 over N_2 and CO_2 over CH_4 as calculated from the initial slope ratio method; (c) IAST adsorption selectivity for CO_2 over N_2 calculated under conditions of 15% CO_2 balanced with N_2 and 313 K; (d) IAST adsorption selectivity for CO_2 over CH_4 as a function of CO_2 concentration calculated under the condition of CO_2/CH_4 mixture gas at 295 K and 1 bar.

between adsorption enthalpy and regeneration energy. It is worth pointing out that the high energy requirement for the regeneration of aqueous amine solution not only stems from the high adsorption enthalpy of chemisorption, but also from the high heat capacity of the aqueous amine solution (approx. 3.5 J g^{-1} K^{-1}),[36] whereas the heat capacity of PPN-6-SO_3NH_4 is less than half. Therefore, the regeneration energy for PPN-6-SO_3NH_4 would be substantially lower than for aqueous amine solution.

One of the common methods to evaluate gas adsorption selectivity involves the use of initial slope ratios (Henry's law constants) for single-component adsorption isotherms.[37] As the name implies, the selectivity is calculated as initial slope (CO_2)/initial slope (N_2) by using their CO_2 and N_2 single-component isotherms. However, it cannot give the real gas selectivity from the binary gas mixture because other selectivity factors are not taken into consideration, such as competition of gas molecules for adsorption sites. Nevertheless, this method is rather useful and convenient to compare the performance between different porous materials for adsorption selectivity. Therefore, we re-measured the gas adsorption isotherms by dosing a very small amount at a time; PPN-6-SO_3NH_4 shows initial-slope-ratio selectivities of 196 (CO_2/N_2) and 40 (CO_2/CH_4) at 295 K (Fig. 2b). These values are higher than some of the top performers in the literature under similar conditions, such as Bio-MOF-11 (CO_2/N_2 selectivity of 75 at 298 K)[38] and BLP-10 (CO_2/CH_4 selectivity of 40 at 273 K).[39] PPN-6-SO_3NH_4 also exhibits very high CO_2/H_2 (1722) and CO_2/CO (109) initial-slope-ratio selectivities (Fig. S13†).

Ideal Adsorption Solution Theory (IAST), developed by Myers and Prausnitz,[40] has been widely used to predict mixture gas adsorption behavior within adsorbents. The inputs to the IAST calculation are the pure-component adsorption isotherms at the temperature of interest, and the output is a prediction of mixture adsorption equilibrium. The accuracy of IAST for estimating component loadings for adsorption of a wide variety of binary mixtures in zeolites has been established with the aid of Configurational-Bias Monte Carlo (CBMC) simulations.[41,42] Specifically, it has previously been applied to predict the separation of CO_2 from N_2 within porous materials.[24,43–49] Under simulated flue gas conditions (15% CO_2, 85% N_2, and 313 K), the calculated IAST for PPN-6-SO_3NH_4 is shown in Fig. 2c. At low pressure, the IAST adsorption selectivity is similar to the CO_2/N_2 pure gas uptake ratio at their partial pressures because most adsorption sites are unsaturated. With the rising pressure and loading, the competition for adsorption sites between CO_2 and N_2 intensifies; therefore the IAST adsorption selectivity rises dramatically due to the much higher affinity of CO_2 to the network. As a result, the IAST adsorption selectivity for PPN-6-SO_3NH_4 is calculated to be 796 at 1 bar, which is more than 10 times the CO_2/N_2 pure gas uptake ratio at their partial pressures (77, Table S3†), and being the highest value at 313 K reported to date. Based on the IAST calculation, the PPN-6-SO_3NH_4 material can accumulate the CO_2 concentration to as high as 99.3% under flue gas conditions (Table S3†).

The CO_2 concentration varies much in natural gas; thus we plot the IAST adsorption selectivity of CO_2 over CH_4 as a function of CO_2 concentration under conditions of 295 K and 1 bar (Fig. 2d). The value is 35 at very low CO_2 concentration; as the CO_2 concentration goes up, the IAST adsorption selectivity goes up rapidly. Under the condition of 50% CO_2 balanced with 50% CH_4, which is commonly used in the literature, the IAST adsorption selectivity for PPN-6-SO_3NH_4 is calculated to be 180, the value being one of the highest among all porous polymers reported so far.[38,39,50,51] With the IAST calculation, we can estimate CO_2 enrichment potential for PPN-6-SO_3NH_4. Based on the IAST calculation, the PPN-6-SO_3NH_4 material can accumulate CO_2 to as high as 99.5% out of a gas mixture of 50% CH_4 and 50% CO_2 (Table S4†).

Recent studies have shown that a temperature swing adsorption (TSA) regeneration process would be significantly less energy consuming than pressure swing adsorption (PSA) and thus, more applicable in a real world application scenario for CO_2 capture from flue gas.[14] To find out the appropriate regeneration temperature, thermogravimetric analysis (TGA) for PPN-6-SO_3NH_4 in air was evaluated, as we can see from Fig. S18,† the sample was heated and kept at 150 °C for 999 min, no obvious weight loss was observed during this period, therefore, it is confident to say that 150 °C is the safe regeneration temperature for this material.

With the thermostability knowledge, we collected CO_2 adsorption isotherms for PPN-6-SO_3NH_4 at different temperatures; Fig. 3 illustrates the working capacity of PPN-6-SO_3NH_4 with a temperature swing over a ΔT from 40 to 150 °C for a flue gas simulant (15% CO_2 balanced with N_2). The amount adsorbed at 40 °C, 0.15 bar (q_1) is 4.8 wt% and upon heating the sample to 150 °C and releasing CO_2 at 1 bar (q_2), only 1.2 wt% is adsorbed, thus generating a working capacity of 3.6 wt% ($q_1 - q_2$) at 150 °C. The working capacity drops to 2.1 wt% if heated up to 120 °C. We could get higher working capacity if purging was applied after heating up, but at the expense of extra energy.

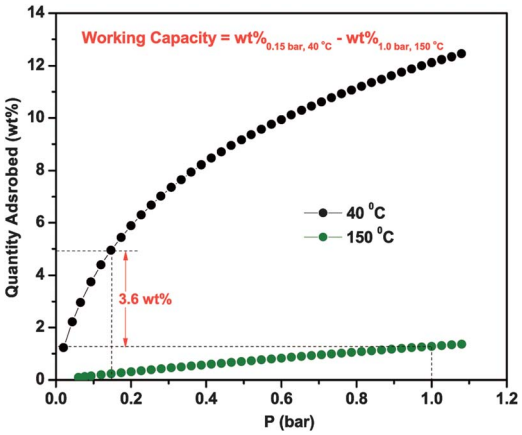

Fig. 3 TSA working capacity for PPN-6-SO_3NH_4 under flue gas conditions (15% CO_2 balanced with N_2), calculated with single gas (CO_2) isotherms at different temperatures, the amount adsorbed at 40 °C, 0.15 bar (q_1) subtracted by the amount adsorbed at 150 °C, 1 bar (q_2).

The working capacity value of PPN-6-SO_3NH_4 is comparable to the working capacity of MEA solutions, which are typically heated under flue gas conditions to about 120 °C and can achieve working capacities of about 2.1 to 5.5 wt% depending on the scrubbing process used in the study.[52,53]

To confirm the high working capacity and dynamic cycling behavior, temperature dependent gravimetric adsorption was studied by using a TGA under flue gas simulant and pure CO_2 conditions. After heating PPN-6-SO_3NH_4 at 150 °C for 30 min, the sample was cooled down and kept at 40 °C for 60 min. As we can see from Fig. S16,† by flowing a flue gas simulant (CO_2/N_2 15 : 85), an experimental mass change of 4.5 wt% (green line) was realized and further cycling experiment does not lead to a visible decrease of the mass change. The value matches very well with the differentiation between the amount of CO_2 adsorbed at 40 °C (4.8 wt%) and 150 °C (0.2 wt%) at 0.15 bar, which emphasizes the capability of PPN-6-SO_3NH_4 as a sorbent to remove CO_2 from flue gas; by flowing pure CO_2, an experimental mass change of 10.4 wt % (black line) was realized and further cycling experiment does not lead to a visible decrease of the mass change. The value is also very close to the differentiation between the amount of CO_2 adsorbed at 40 °C (12.1 wt%) and 150 °C (1.2 wt%) at 1.0 bar.

To verify the separation results calculated by IAST we measured the separation of CO_2 from the CO_2/N_2 binary mixture in a fixed-bed (345 mg of PPN-6-SO_3NH_4 packed in a stainless steel tube with an inner diameter of 8 mm and a length of 80 mm). Breakthroughs of the following gas composition have been measured (pure CO_2, 50% CO_2/50% N_2, 15% CO_2/85% N_2). The breakthrough was run at environmental pressure and 40 °C as well as 23 °C for each gas composition two times. We measured the bed temperature *in situ* at the end of the packed bed, having a thermocouple sticking into the material. Furthermore we measured the pressure drop over the packed bed to ensure a low pressure drop (see ESI†).

The adsorbent was first activated by heating to 95 °C in helium with a flow rate of 20 mL min^{-1} for 24 hours. After that breakthrough experiments were carried out.

For all experiments the pressure drop was lower than 10 mbar and was neglected for further analysis. The temperature reached a constant level before reaching the continuous state (Fig. 4, bottom) of the experiment; therefore we made the assumption of a homogeneous adsorption temperature. We evaluated the CO_2 uptake from the breakthrough data as explained in the ESI.† The empty volume was measured with an argon/helium experiment as can be found in the ESI† as well.

We obtained clear breakthrough curves from the experimental data (Fig. 4, top). In the example we show the breakthrough of a 15% CO_2/85% N_2 gas mixture at 40 °C and 1 bar. As expected the curves indicate a highly selective adsorption of CO_2 over N_2 in the framework.

The measured breakthrough curve (Fig. 4) can be divided into three stages. Stage 1 (120–250 s), both CO_2 and N_2 fill the system while He will be pressed out of the empty volume. Stage 2 (starting from 250 s), while the breakthrough of N_2 is detected the CO_2 concentration in the outlet remains zero because it is captured by the adsorbents. Stage 3 (>700 s), after the breakthrough, the CO_2 concentration reaches the input composition.

According to the breakthrough curve at 40 °C, 1 bar, and 15% CO_2, we can calculate the CO_2 uptake of PPN-6-SO_3NH_4 to 1.15 $mmol_{CO2}$ per g, which is in good agreement with the pure gas CO_2 adsorption data (1.13 $mmol_{CO2}$ per g).

Fig. 5 demonstrates good agreement between adsorption isotherms of pure CO_2 on PPN-6-SO_3NH_4 and the calculated CO_2 adsorption capacities using the breakthrough experimental data. The measured results are consistent with the predicted solution (IAST calculation) that the CO_2 adsorption capacity is not dependent on the N_2 fraction in the gas phase. Selectivity was not calculated from the breakthrough data because the necessary *in situ* flow measurement in the outlet of the system has not been integrated in our measurement setup.

The CO_2 saturated PPN-6-SO_3NH_4 was subjected to an argon purge flow of 10 mL min^{-1} at 90 °C. After approximately 100 minutes, no CO_2 was detected in the effluent stream. Successive regeneration experiments show that PPN-6-SO_3NH_4 retains almost 100% of its intrinsic capture capacity after mild regeneration.

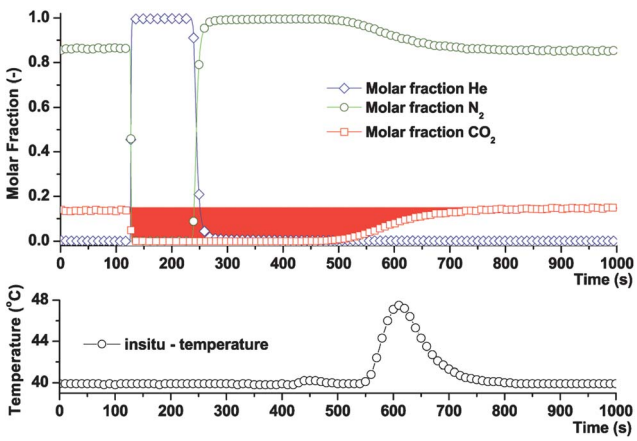

Fig. 4 (Top) CO_2/N_2 (15 : 85) breakthrough curves at 40 °C for the PPN-6-SO_3NH_4 under dry conditions. The flow rate is 10 mL min^{-1}. (Bottom) *In situ* temperature at the end of the packed bed.

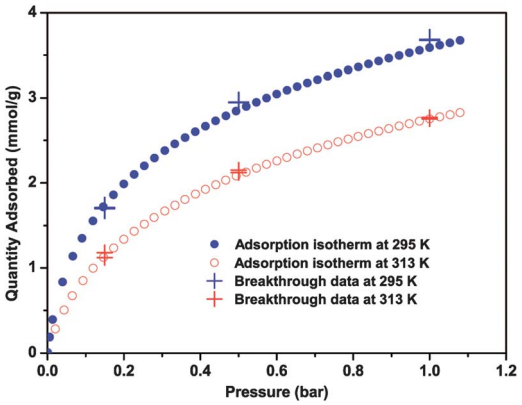

Fig. 5 (●) Pure CO_2 adsorption isotherm at 295 K; (○) pure CO_2 adsorption isotherm at 313 K; (+) CO_2 adsorption capacity at 295 K, calculated from breakthrough curves with 15/85 CO_2/N_2, 50/50 CO_2/N_2, pure CO_2 as feeding gas, respectively. (+) CO_2 adsorption capacity at 313 K, calculated from breakthrough curves with 15/85 CO_2/N_2, 50/50 CO_2/N_2, pure CO_2 as feeding gas, respectively.

Further cycling experiment does not lead to visible reduction of the capture capacity. The results signify that PPN-6-SO_3NH_4 can achieve a high-capacity separation under mild conditions for regeneration. High CO_2 capture capacity and separation selectivity, easy handling and facile regeneration ability are desirable and indispensable properties for practical CO_2 capture applications. Hence, the dynamic results also confirm that PPN-6-SO_3NH_4 is extremely selective for adsorbing CO_2 over N_2 and represents a major advance in CO_2 separation capacity.

Conclusions

We have shown that we can rationally build porous polymer networks with multiple adsorption sites for binding CO_2 under ambient conditions. PPN-6-SO_3NH_4 was demonstrated to have exceptionally high CO_2 capacity at low pressures and CO_2 over N_2 selectivity by using a variety of methods. Given the outstanding physicochemical stability (Fig. S20†) and mild regeneration requirements, it has great potential for practical application in a post-combustion CO_2 capture technology. Although very efficient, aqueous amine solutions have drawbacks such as boil-off, fouling of the equipment, being oxidized especially at elevated temperatures, *etc.* Therefore, it was viable for PPN-6-SO_3NH_4 to edge out aqueous amine solutions if we could bring down the production cost of scale-up, which, as a matter of fact, would ultimately be linked to recyclability and lifetime, and cannot easily be calculated from lab-scale experiments.

Acknowledgements

This work was supported by the U.S. Department of Energy as part of the Center for Gas Separations Relevant to Clean Energy Technologies, an Energy Frontier Research Center funded by the U.S. DOE, Office of Science, Office of Basic Energy Sciences under Award Number (DE-SC0001015 and DE-AR0000073), the National Science Foundation (NSF CBET-0930079), and the Welch Foundation (A-1725).

Notes and references

1 J. D. Figueroa, T. Fout, S. Plasynski, H. McIlvried and R. D. Srivastava, *Int. J. Greenhouse Gas Control*, 2008, **2**, 9–20.
2 N. MacDowell, N. Florin, A. Buchard, J. Hallett, A. Galindo, G. Jackson, C. S. Adjiman, C. K. Williams, N. Shah and P. Fennell, *Energy Environ. Sci.*, 2010, **3**, 1645–1669.
3 T. Lewis, M. Faubel, B. Winter and J. C. Hemminger, *Angew. Chem., Int. Ed.*, 2011, **50**, 10178–10181.
4 Y.-S. Bae and R. Q. Snurr, *Angew. Chem., Int. Ed.*, 2011, **50**, 11586–11596.
5 J.-R. Li, R. J. Kuppler and H.-C. Zhou, *Chem. Soc. Rev.*, 2009, **38**, 1477–1504.
6 J.-R. Li, Y. Ma, M. C. McCarthy, J. Sculley, J. Yu, H.-K. Jeong, P. B. Balbuena and H.-C. Zhou, *Coord. Chem. Rev.*, 2011, **255**, 1791–1823.
7 D. M. D'Alessandro, B. Smit and J. R. Long, *Angew. Chem., Int. Ed.*, 2010, **49**, 6058–6082.
8 Q. Wang, J. Luo, Z. Zhong and A. Borgna, *Energy Environ. Sci.*, 2011, **4**, 42–55.
9 N. Hedin, L. Chen and A. Laaksonen, *Nanoscale*, 2010, **2**, 1819–1841.
10 T. C. Drage, C. E. Snape, L. A. Stevens, J. Wood, J. Wang, A. I. Cooper, R. Dawson, X. Guo, C. Satterley and R. Irons, *J. Mater. Chem.*, 2012, **22**, 2815–2823.
11 R. Dawson, A. I. Cooper and D. J. Adams, *Polym. Int.*, 2013, **62**, 345–352.
12 R. Dawson, A. I. Cooper and D. J. Adams, *Prog. Polym. Sci.*, 2012, **37**, 530–563.
13 Z. Xiang, X. Zhou, C. Zhou, S. Zhong, X. He, C. Qin and D. Cao, *J. Mater. Chem.*, 2012, **22**, 22663–22669.
14 J. A. Mason, K. Sumida, Z. R. Herm, R. Krishna and J. R. Long, *Energy Environ. Sci.*, 2011, **4**, 3030–3040.
15 A. C. Kizzie, A. G. Wong-Foy and A. J. Matzger, *Langmuir*, 2011, **27**, 6368–6373.
16 H. Furukawa, N. Ko, Y. B. Go, N. Aratani, S. B. Choi, E. Choi, A. Ö. Yazaydin, R. Q. Snurr, M. O'Keeffe, J. Kim and O. M. Yaghi, *Science*, 2010, **329**, 424–428.
17 O. K. Farha, A. Özgür Yazaydın, I. Eryazici, C. D. Malliakas, B. G. Hauser, M. G. Kanatzidis, S. T. Nguyen, R. Q. Snurr and J. T. Hupp, *Nat. Chem.*, 2010, **2**, 944–948.
18 T. Ben, H. Ren, S. Ma, D. Cao, J. Lan, X. Jing, W. Wang, J. Xu, F. Deng, J. M. Simmons, S. Qiu and G. Zhu, *Angew. Chem., Int. Ed.*, 2009, **48**, 9457–9460.
19 D. Yuan, W. Lu, D. Zhao and H.-C. Zhou, *Adv. Mater.*, 2011, **23**, 3723–3725.
20 U. Stoeck, S. Krause, V. Bon, I. Senkovska and S. Kaskel, *Chem. Commun.*, 2012, **48**, 10841–10843.
21 T. A. Makal, J.-R. Li, W. Lu and H.-C. Zhou, *Chem. Soc. Rev.*, 2012, **41**, 7761–7779.
22 S. Matteucci, Y. Yampolskii, B. D. Freeman and I. Pinnau, in *Materials Science of Membranes for Gas and Vapor Separation*, John Wiley & Sons, Ltd, 2006, pp. 1–47.
23 G. Aguilar-Armenta, G. Hernandez-Ramirez, E. Flores-Loyola, A. Ugarte-Castaneda, R. Silva-Gonzalez, C. Tabares-Munoz, A. Jimenez-Lopez and E. Rodriguez-Castellon, *J. Phys. Chem. B*, 2001, **105**, 1313–1319.

24 H. A. Patel, S. Hyun Je, J. Park, D. P. Chen, Y. Jung, C. T. Yavuz and A. Coskun, *Nat. Commun.*, 2013, **4**, 1357.
25 A. P. Katsoulidis and M. G. Kanatzidis, *Chem. Mater.*, 2011, **23**, 1818–1824.
26 H. A. Patel and C. T. Yavuz, *Chem. Commun.*, 2012, **48**, 9989–9991.
27 S. J. Garibay, M. H. Weston, J. E. Mondloch, Y. J. Colon, O. K. Farha, J. T. Hupp and S. T. Nguyen, *CrystEngComm*, 2013, **15**, 1515–1519.
28 M. G. Rabbani, A. K. Sekizkardes, O. M. El-Kadri, B. R. Kaafarani and H. M. El-Kaderi, *J. Mater. Chem.*, 2012, **22**, 25409–25417.
29 C. G. Bezzu, M. Carta, A. Tonkins, J. C. Jansen, P. Bernardo, F. Bazzarelli and N. B. McKeown, *Adv. Mater.*, 2012, **24**, 5930–5933.
30 R. Dawson, D. J. Adams and A. I. Cooper, *Chem. Sci.*, 2011, **2**, 1173–1177.
31 W. Lu, J. P. Sculley, D. Yuan, R. Krishna, Z. Wei and H.-C. Zhou, *Angew. Chem., Int. Ed.*, 2012, **51**, 7480–7484.
32 W. Lu, D. Yuan, D. Zhao, C. I. Schilling, O. Plietzsch, T. Muller, S. Bräse, J. Guenther, J. Blümel, R. Krishna, Z. Li and H.-C. Zhou, *Chem. Mater.*, 2010, **22**, 5964–5972.
33 W. Lu, D. Yuan, J. Sculley, D. Zhao, R. Krishna and H.-C. Zhou, *J. Am. Chem. Soc.*, 2011, **133**, 18126–18129.
34 D. Britt, H. Furukawa, B. Wang, T. G. Glover and O. M. Yaghi, *Proc. Natl. Acad. Sci. U. S. A.*, 2009, **106**, 20637–20640.
35 S. Keskin, T. M. van Heest and D. S. Sholl, *ChemSusChem*, 2010, **3**, 879–891.
36 R. H. Weiland, J. C. Dingman and D. B. Cronin, *J. Chem. Eng. Data*, 1997, **42**, 1004–1006.
37 K. Kent, in *Albright's Chemical Engineering Handbook*, CRC Press, 2008, pp. 1119–1171.
38 J. An, S. J. Geib and N. L. Rosi, *J. Am. Chem. Soc.*, 2009, **132**, 38–39.
39 T. E. Reich, S. Behera, K. T. Jackson, P. Jena and H. M. El-Kaderi, *J. Mater. Chem.*, 2012, **22**, 13524–13528.
40 A. L. Myers and J. M. Prausnitz, *AIChE J.*, 1965, **11**, 121–127.
41 R. Krishna, S. Calero and B. Smit, *Chem. Eng. J.*, 2002, **88**, 81–94.
42 R. Krishna and J. M. van Baten, *Chem. Eng. J.*, 2007, **133**, 121–131.
43 Y. S. Bae, O. K. Farha, J. T. Hupp and R. Q. Snurr, *J. Mater. Chem.*, 2009, **19**, 2131–2134.
44 A. O. Yazaydin, A. I. Benin, S. A. Faheem, P. Jakubczak, J. J. Low, R. R. Willis and R. Q. Snurr, *Chem. Mater.*, 2009, **21**, 1425–1430.
45 B. S. Zheng, J. F. Bai, J. G. Duan, L. Wojtas and M. J. Zaworotko, *J. Am. Chem. Soc.*, 2011, **133**, 748–751.
46 J. M. Simmons, H. Wu, W. Zhou and T. Yildirim, *Energy Environ. Sci.*, 2011, **4**, 2177–2185.
47 R. Krishna and J. M. van Baten, *Phys. Chem. Chem. Phys.*, 2011, **13**, 10593–10616.
48 Y. Belmabkhout and A. Sayari, *Adsorption*, 2009, **15**, 318–328.
49 A. Goj, D. S. Sholl, E. D. Akten and D. Kohen, *J. Phys. Chem. B*, 2002, **106**, 8367–8375.
50 Y.-S. Bae, B. G. Hauser, O. K. Farha, J. T. Hupp and R. Q. Snurr, *Microporous Mesoporous Mater.*, 2011, **141**, 231–235.
51 Y.-S. Bae, O. K. Farha, J. T. Hupp and R. Q. Snurr, *J. Mater. Chem.*, 2009, **19**, 2131–2134.
52 K. Sumida, D. L. Rogow, J. A. Mason, T. M. McDonald, E. D. Bloch, Z. R. Herm, T.-H. Bae and J. R. Long, *Chem. Rev.*, 2011, **112**, 724–781.
53 A. N. M. Peeters, A. P. C. Faaij and W. C. Turkenburg, *Int. J. Greenhouse Gas Control*, 2007, **1**, 396–417.

